IOP Publishing | International Atomic Energy Agency Nuclear Fusion

Nucl. Fusion **61** (2021) 106021 (8pp) https://doi.org/10.1088/1741-4326/ac189d

Isotope dependence of beta-induced Alfvén eigenmode (BAE) and low frequency mode (LFM) stability in DIII-D

W.W. Heidbrink[1,*], G.J. Choi[1], M.A. Van Zeeland[2], M.E. Austin[3], G.H. Degrandchamp[1], D.A. Spong[4], A. Bierwage[5], N.A. Crocker[6], X.D. Du[2], P. Lauber[7], Z. Lin[1] and G.R. McKee[8]

[1] University of California, Irvine, CA, United States of America
[2] General Atomics, San Diego, CA, United States of America
[3] University of Texas, Austin, TX, United States of America
[4] Oak Ridge National Laboratory, TN, United States of America
[5] National Institutes for Quantum and Radiological Science and Technology, Rokkasho Fusion Institute, Aomori 039-3212, Japan
[6] University of California, Los Angeles, CA, United States of America
[7] Max Planck Institute for Plasma Physics, Boltzmannstr. 2, 85748 Garching, Germany
[8] University of Wisconsin, Madison, WI, United States of America

E-mail: Bill.Heidbrink@uci.edu

Received 25 May 2021, revised 17 July 2021
Accepted for publication 28 July 2021
Published 21 September 2021

Abstract

The stability of beta-induced Alfvén eigenmodes (BAE) and the low frequency modes (LFMs) that were formerly called beta-induced Alfvén-acoustic eigenmodes is discussed. After a brief summary of previous publications on the stability in DIII-D beam-heated, reversed-shear, deuterium plasmas with deuterium neutral beam injection (NBI), new observations in mixed hydrogen and deuterium plasmas are reported. With deuterium NBI, BAEs are at least as unstable in mixed-species plasmas as in deuterium plasmas; however, with hydrogen NBI, the BAEs are stable. In contrast, the LFMs are unaffected by changes in beam species, consistent with the previous observation that LFMs are not driven by high-energy beam ions. As predicted by theory, the LFMs appear more unstable in mixed species plasmas than in pure deuterium discharges.

Keywords: Alfven eigenmode, fast ions, tokamak

(Some figures may appear in colour only in the online journal)

1. Introduction

The beta-induced Alfvén eigenmode (BAE) [1] and beta-induced Alfvén-acoustic eigenmode (BAAE) [2] are two instabilities with frequencies below that of toroidal Alfvén eigenmodes (TAEs) [3] and reversed shear Alfvén eigenmodes (RSAE) [4]. Both the BAE [1, 5] and the BAAE [6] have been implicated in degraded fast-ion confinement. Although much attention has been devoted to predictions of TAE stability in future devices, these potentially dangerous lower-frequency modes have received far less attention. The purpose of the dedicated DIII-D experiment summarized here is to provide additional information on BAE and BAAE stability, with the ultimate goal of providing well-validated stability predictions for ITER and other future devices. More complete documentation appears in two longer articles, one on the BAE [7] and one on the instability that was formerly identified as the BAAE that is now called a low frequency mode (LFM) [8]. In addition, a paper on gyrokinetic simulations of these discharges was also recently published [9]. The earlier experimental work

* Author to whom any correspondence should be addressed.

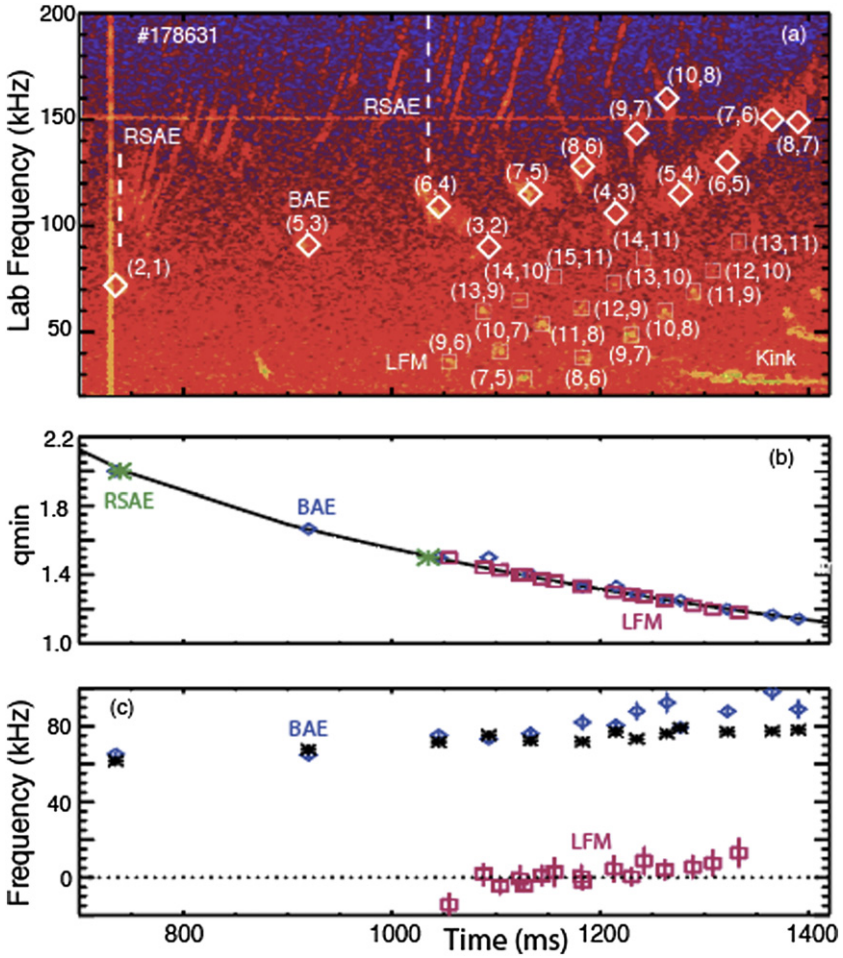

Figure 1. (*a*) Cross-power spectrogram in the reference shot of the dedicated experiment for ECE channels between normalized minor radii of 0.29–0.44. The BAEs (diamond) and LFMs (squares) are labeled by their poloidal and toroidal (m, n) numbers. The dashed vertical lines are the times of $q_{\min} = 2$ and 1.5 crossings inferred from the RSAE activity on ECE and interferometer signals. (*b*) Measured $q_{\min}$ from EFIT reconstructions vs time. The RSAE (*), BAE (diamond), and LFM (square) symbols represent the values of m/n shown on the spectrogram. (*c*) Inferred frequencies in the plasma frame for BAEs (diamond) and LFMs (squares) from the formula $f_{\rm pl} = f_{\rm lab} - nf_{\rm rot}$, where $f_{\rm lab}$ is the measured frequency and $f_{\rm rot}$ is the rotation frequency at the peak of the radial eigenfunction. The error bars represent the uncertainty in the Doppler shift correction $nf_{\rm rot}$. The BAE accumulation frequency (*) is also shown. Reproduced courtesy of IAEA. Figure from [7]. Copyright (2021) IAEA.

is summarized in the remainder of this section. New data and theory for plasmas with mixed concentrations of hydrogen and deuterium appear in sections 2 and 3, respectively.

The dedicated experiment is conducted during the current ramp when the q profile is weakly reversed. Injection of ~ 80 keV deuterium neutral beams produces an anisotropic population of sub-Alfvénic fast ions that can potentially drive instability. Prior to the time of interest, the neutral beam injection (NBI) and electron cyclotron heating (ECH) patterns remain identical on successive shots; consequently, the q profile and mode activity are highly reproducible shot-to-shot. At the time of interest, the beam and/or ECH patterns are modified to investigate the effect of fast-ion and thermal driving gradients on mode stability.

During the time of interest, three different types of instability occur: RSAEs, BAEs, and LFMs (figure 1(*a*)). Electron cyclotron emission (ECE) data (figure 2) shows that all three modes have radial eigenfunctions that peak near $q_{\min}$, although there is some tendency for the BAE to peak closer to the magnetic axis (in the negative magnetic shear region) than the other two instabilities. All three modes depend sensitively on the value of $q_{\min}$, which steadily decreases during the time of interest (figure 1(*b*)). RSAEs exhibit the 'Alfvén cascades' first reported on JET [4]: at rational values of $q_{\min}$, RSAEs with different toroidal mode numbers n have similar frequencies in the plasma frame, then the frequencies sweep upward at different rates as time evolves. (The cascades when $q_{\min} = 2$ and 1.5 are marked in figure 1(*a*).) In contrast, the LFMs are only unstable when $q_{\min}$ is close to a rational value; as a result, the LFMs appear in ascending patterns reminiscent of Christmas lights. The BAEs are also unstable when $q_{\min}$ approaches a rational value, although their appearance is less regular than for the LFMs (figure 1(*b*)). Another difference between the BAEs and the other instabilities is that, on a millisecond timescale, the BAE frequency chirps rapidly by $\sim 10\%$, while the frequencies of LFMs and RSAEs hardly changes. The toroidal rotation frequency at $q_{\min}$ and the temporal evolution of $q_{\min}$ are both known accurately, so the pattern of unstable BAEs and LFMs vs time enables unique identification of poloidal

and toroidal mode numbers (m, n) for each mode (figure 1(a)). The LFMs do not appear on magnetics so, for them, it is not possible to use the toroidal magnetics array to check the n number assignments; however, a set of discharges with high-quality beam emission spectroscopy data confirm the correctness of the poloidal mode number assignments [8]. For the BAEs, data from the toroidal magnetics array confirm the toroidal mode number assignments for $n = 1$–3 [7].

Figure 1(c) shows the inferred frequencies in the plasma frame. After correction for the Doppler shift, the LFM frequencies in the plasma frame are comparable to ion diamagnetic frequencies and are significantly lower than the frequency of the beta-induced Alfvén-acoustic gap in the continuum. For this reason, the modes are no longer identified as BAAEs [8]. The frequencies of the BAEs are close (typically within 10%) to the geodesic acoustic mode (GAM) frequency [10], which is also the BAE accumulation point of the Alfvén continuum,

$$f_{\mathrm{GAM}} = \left[\frac{1}{2\pi^2 m_{\mathrm{i}} R_0^2}\left(T_{\mathrm{e}} + \frac{7}{4}T_{\mathrm{i}}\right)\left(1 + \frac{1}{2q^2}\right)\frac{2}{\kappa^2 + 1}\right]^{1/2}, \quad (1)$$

where m_{i} is the ion mass and R_0 is the magnetic axis.

The principal results of the dedicated experiment are illustrated in figure 3. When the beams turn off, the BAE activity ceases in a time that is much shorter than the ~ 100 ms slowing-down time. In discharges where all of the beams turn off, RSAE activity also ceases, although it generally persists longer than BAE activity. In contrast, the activity in the lower frequency band persists unabated even in the absence of beam injection. (For the example of figure 3, even though T_{e} and ∇T_{e} at q_{min} hardly change, the LFM amplitude roughly doubles in amplitude when the beams are off.) Irrespective of the beam injection pattern, unstable LFMs are observed in all discharges of the dedicated experiment with sustained values of electron temperature T_{e} [8].

The BAEs in the dedicated experiment are driven by co-passing fast ions that are injected by the tangential neutral beam sources [7]. When perpendicular beams substitute for tangential beams, the BAEs quickly cease. The BAEs are unstable when the condition for resonant interaction between recently deposited tangential beams and the mode is satisfied. As q_{min} evolves, the resonances shift away from the anisotropic fast-ion population in phase space; these shifts appear to be the primary factor that determine the duration of instability for each individual BAE [7].

Three sets of data have been assembled for deuterium plasmas [7, 8]. For all three databases, in each time interval, the mode activity is classified as 'stable', 'marginal', or 'unstable' in the LFM, BAE, RSAE, and TAE frequency bands. Also, all three databases are restricted to the first two seconds of the discharge, when the evolving q profile facilitates mode identification. All databases contain kinetic profile data and data extracted from equilibrium reconstructions. The largest database contains over 2000 entries from over 1000 different discharges and spans a very wide range of plasma parameters. A second database is from the 20 shots of the dedicated experiment and contains additional information on mode amplitudes and the fast-ion distribution function. The third database is from a search for unstable LFMs in discharges without NBI.

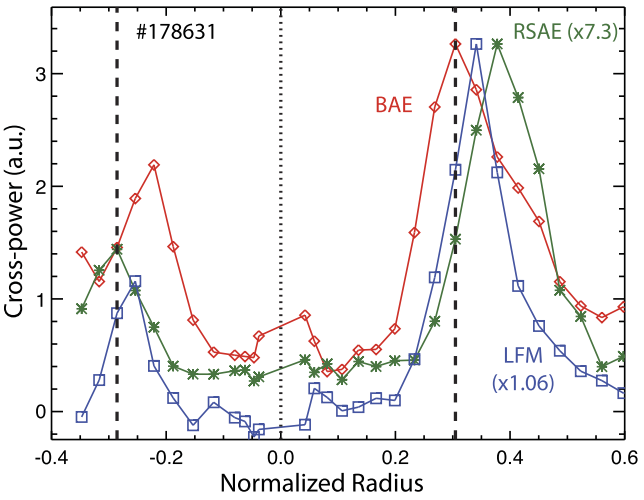

Figure 2. Comparison of the RSAE (*), BAE (diamond), and LFM (square) radial eigenfunctions measured by ECE in the same discharge as figure 1. To facilitate comparison, the RSAE (LFM) spectra have been multiplied by 7.3 (1.06). The cross-power is taken between adjacent ECE channels. The abscissa is the normalized square root of the toroidal flux. The vertical dashed line represents the approximate location of q_{min}; the dotted line is the magnetic axis. The LFM is from 1144 ms, while the RSAE and BAE are from 1125 ms.

All three databases support the same conclusions. LFMs are unstable most often in plasmas with high electron temperature but relatively low beta (figure 4(a)). In contrast, unstable BAEs appear most often in high beta plasmas (figure 4(b)). The dependence on T_{e} (or its gradient) and on beta are the strongest dependencies in the databases for LFMs [8]. For BAEs, the strongest dependencies are on beta and beam parameters [7].

The LFM observations motivated new analytical theory that appears in [8]. A reactive instability of Alfvénic polarization that is excited by steep electron temperature gradients near q_{min} has properties that are consistent with the experiment. Linear simulations of the reference case have been performed by the gyrofluid code FAR3d [11], the linear gyrokinetic code LIGKA [12], and the gyrokinetic code GTC [9]. Both FAR3d and GTC find unstable modes near q_{min} with frequencies comparable to LFM frequencies. In GTC, the mode is unstable in the absence of fast ions. As in experiment, the growth rate calculated by GTC increases with increasing T_{e}. A detailed report on the GTC simulations appears in [9]. FAR3d, LIGKA, and GTC all find unstable fast-ion driven modes that are located near q_{min} with frequencies comparable to the experimental BAEs [7]. In the GTC simulations, the BAE frequency is sensitive to the number of fast ions in a manner suggestive of an energetic particle mode, which may explain the frequency chirping observed experimentally. One difference from the experiment is that the growth rate calculated by both FAR3d [7] and GTC [9] is rather insensitive to q_{min} while, in experiment, a given BAE is only unstable over a small range of q_{min}. All of the simulations to date employ an isotropic distribution function and it is well established experimentally that BAE stability is quite sensitive to the direction of the beam injection, so the likely explanation for this discrepancy is the use of isotropic distribution functions in the simulations. Simulations

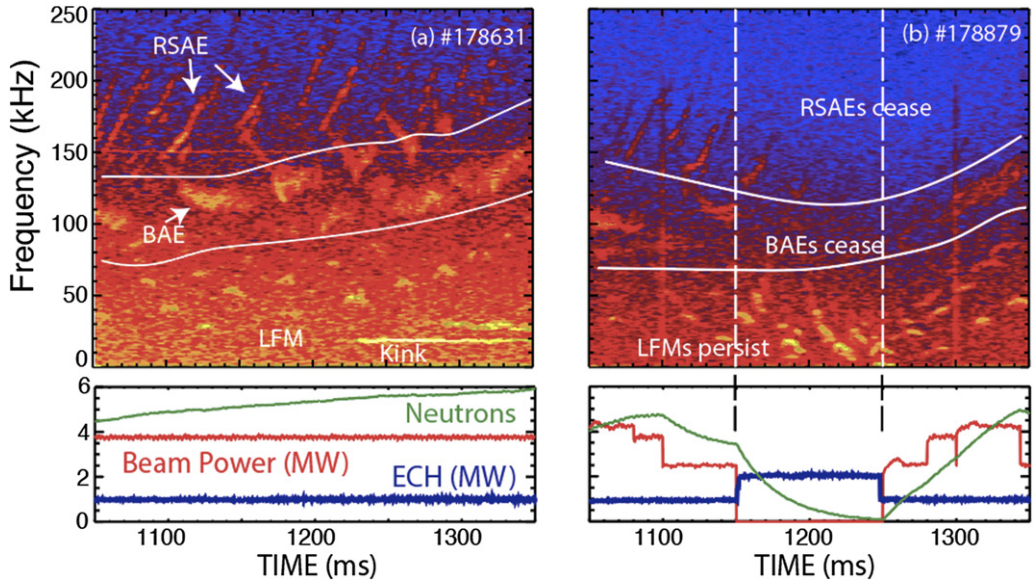

Figure 3. Cross-power ECE spectrograms in (*a*) the reference shot and (*b*) a discharge where the neutral beams temporarily turn off. The white lines are guides to the eye that separate the RSAE, BAE, and LFM frequency bands. When the beam power turns off, BAE activity ceases first, then RSAE activity ceases; the LFM activity persists throughout. (Because the plasma rotation slows when the beams are off, the Doppler-shifted LFM frequencies drop, then increase again when beam injection resumes.) The lower panels show the beam and ECH power traces and the neutron rate (in units of 10^{14} n s^{-1}).

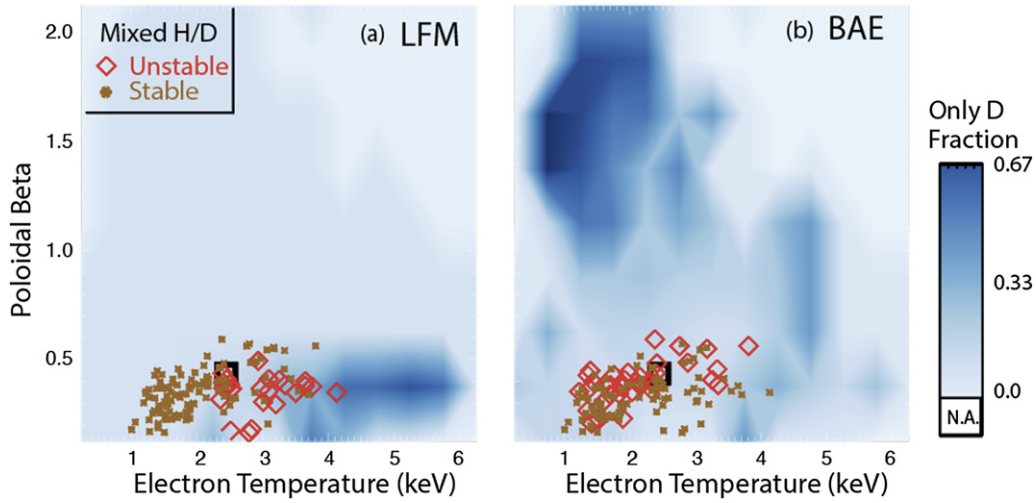

Figure 4. Stability diagrams for (*a*) LFMs and (*b*) BAEs vs central T_e and β_p. The shading indicates the fraction of entries with unstable activity per temperature-beta bin in the large database of deuterium discharges. The location of the deuterium reference shot (figure 1) is identified by the square. Stable (*) and unstable (diamond) conditions observed in mixed-species discharges are also indicated. White regions indicate a portion of parameter space without entries.

with realistic anisotropic distribution functions are planned as future work.

2. Observations in mixed species plasmas

DIII-D recently completed several experiments with the injection of both hydrogen and deuterium beams into plasmas with significant thermal hydrogen concentrations. Although none of these plasmas are an exact match of the conditions of the dedicated deuterium experiment, many have a similar phase with combined ECH and beam injection into a plasma with a weakly reversed q profile, as in the dedicated experiment. Figure 5 shows an example.

To measure the deuterium concentration, short deuterium beam 'blips' from one of the beams injected into most discharges of the 'isotope campaign'. The central value of n_d is estimated from the rate of rise of the neutron emission [13]. The deuterium concentration n_d/n_e in the available discharges ranges between 4%–74%. A new database of 83 'isotope campaign' shots contains the deuterium concentration, the

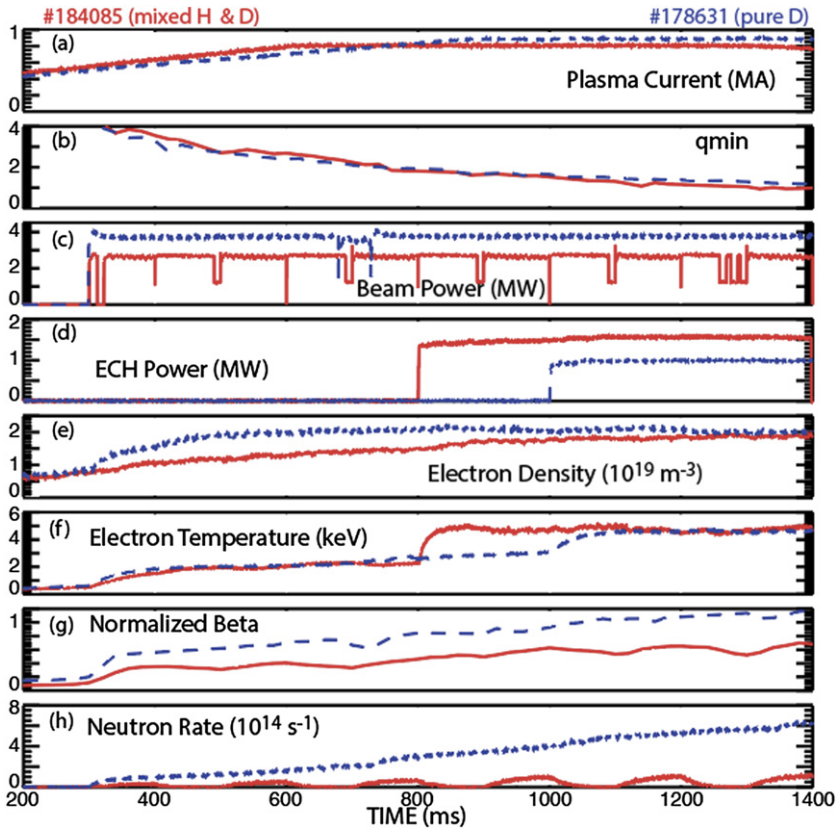

Figure 5. Time evolution of (*a*) plasma current I_p, (*b*) q_{min}, (*c*) beam power, (*d*) ECH power, (*e*) line-averaged electron density $\bar{n}_e$, (*f*) central electron temperature T_e, (*g*) normalized beta β_N and (*h*) measured neutron rate in the dedicated deuterium experiment (dashed) and in the mixed-species discharge shown in figure 6 (solid).

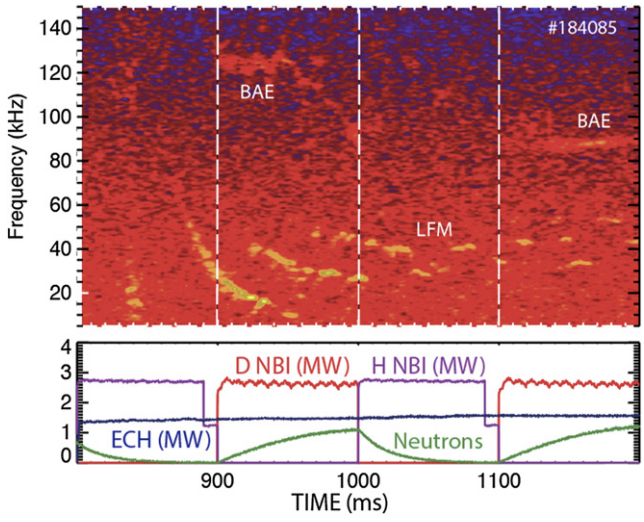

Figure 6. Cross-power ECE spectrogram from a discharge with approximately 50% hydrogen and alternating injection of hydrogen and deuterium neutral beams in the discharge of figure 5. The units of the neutron signal are 10^{14} n s^{-1}. Magnetics data show that the unstable BAE at 1160 ms has a toroidal mode number $n = 2$. Toroidal field $B_T = 2.0$ T.

power injected by deuterium or hydrogen beams, and all of the information in the large deuterium database.

Many discharges have unstable LFMs, BAEs, or both. Figure 6 shows an example. Notice that the BAEs only appear during deuterium NBI; hydrogen injection did not destabilize BAEs in any discharge in the recent isotope campaign. In contrast, as expected, the occurrence of unstable LFMs is independent of beam type.

Table 1. Number of stable and unstable LFM and BAE entries in the deuterium and mixed-species databases.

Database	LFM: unstable/stable	BAE: unstable/stable
Deuterium	43/1312 (3.3%)	137/1174 (11.7%)
Mixed H/D	25/113 (22%)	37/124 (30%)

Comparison of the new database to the large deuterium database illuminates general trends. For the LFM, instability requires $T_e > 2$ keV and modest poloidal beta, just as in deuterium discharges (figure 4(*a*)). (Actually, owing to limited hydrogen beam power and poorer confinement in hydrogen, all of the discharges in the isotope campaign have relatively low β_p in the first two seconds of the discharge.) For the BAE, as in deuterium discharges, the occurrence of instability correlates positively with β_p but is uncorrelated with T_e (figure 4(*b*)). For these isotope campaign shots, the β_p dependence may actually reflect an underlying dependence on deuterium beam power P_B^D, as β_p and P_B^D are strongly correlated in this dataset. Indeed, unstable BAEs are not observed unless P_B^D exceeds 2.0 MW.

It appears that both the BAE and the LFM are more unstable in the mixed species plasmas. Table 1 compares the number

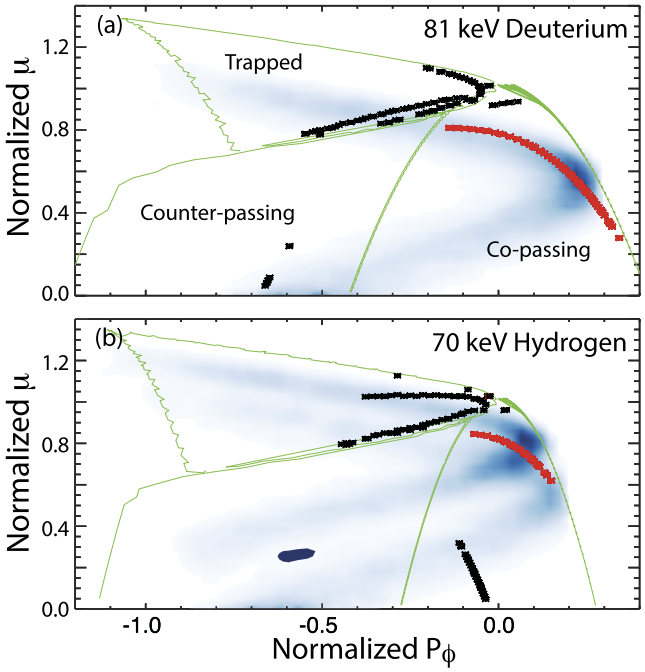

Figure 7. Location in phase space of beam deposition (shading) and resonances (*) for (*a*) 81 keV deuterium fast ions and (*b*) 70 keV hydrogen fast ions at 1160 ms in the discharge of figure 6. In both panels, resonances with the $n = 2$, 88 kHz BAE are shown, with the $p = m - 1 = 2$ resonance highlighted in red. The ordinate is the normalized magnetic moment $\mu B_0/W$, the abscissa is the toroidal canonical angular momentum normalized to the poloidal flux at the last closed flux surface, and the thin lines demarcate topological boundaries.

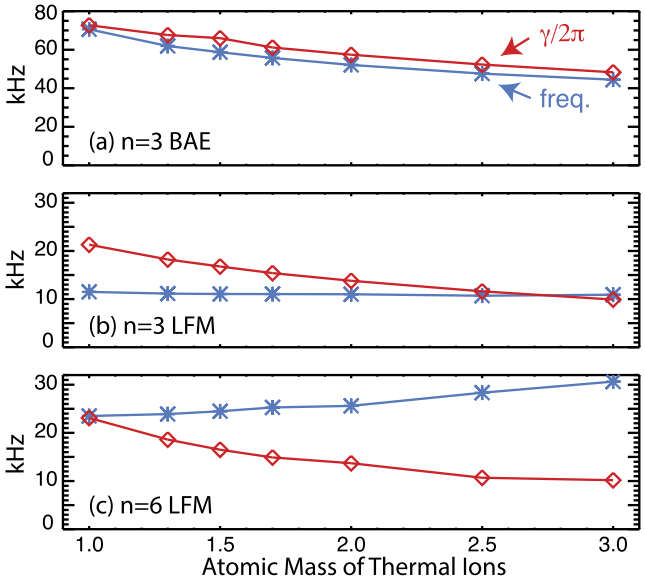

Figure 8. Thermal ion mass dependence of the growth rate (diamond) and mode frequency (*) for linear GTC simulations of (*a*) the $n = 3$ BAE, (*b*) the $n = 3$ LFM, and (*c*) the $n = 6$ LFM. Each simulation is based on the modeling described in [9] of discharge #178631, i.e. with deuterium fast ions for the BAE simulations and without any fast ions for the LFM simulations.

of stable and unstable cases in the pure-deuterium database to the numbers in the recent mixed-species discharges. (The deuterium database is constrained to span the same range of T_e and β_p as the mixed-species entries.) For the LFM, only 3.3% of the entries are unstable in the deuterium database but 22% are unstable in the mixed species database. For the BAE, 12% are unstable in the deuterium database but 30% are unstable in the mixed-species database. However, for both modes, discharges with roughly equal hydrogen and deuterium concentrations are just as unstable as discharges with very high hydrogen concentrations.

3. Theoretical dependence of growth rate on stability

According to the analytical theory presented in [8], the LFM instability threshold is given by

$$(2/qs)(\sqrt{\epsilon}/c_0)^{1/2}|\delta\widehat{W}_f + \delta\widehat{W}_{kt}| > |\omega_{*pi} - \langle\bar{\omega}_{di}\rangle|/\omega_A. \quad (2)$$

Here, s is the magnetic shear, ϵ is the inverse aspect ratio, c_0 is a constant, $\delta\widehat{W}_f$ and $\delta\widehat{W}_{kt}$ are normalized potential energies due to, respectively, the incompressible fluid and the magnetically trapped particles, ω_{*pi} is the thermal ion diamagnetic drift frequency, $\langle\bar{\omega}_{di}\rangle$ is the average thermal-ion precession frequency, and ω_A is the Alfvén frequency. For the conditions of the experiment, the dominant drive term on the left-hand side of the equation is due to thermal electrons, so the drive term is hardly affected by changes in either thermal-ion mass or beam-ion mass; moreover, the sub-dominant ion contributions to $\delta\widehat{W}_f$ and $\delta\widehat{W}_{kt}$ enter via the so-called ideal region where inertia does not appear, only pressure. On the right-hand side, the ion diamagnetic frequency and thermal precession frequencies ω_{*pi} and $\langle\bar{\omega}_{di}\rangle$ are independent of mass but the Alfvén frequency scales as $m_i^{-1/2}$, so the right-hand side decreases when the ion species changes from deuterium to hydrogen. Thus, equation (2) predicts that LFMs should be more unstable in mixed-species plasmas, as observed experimentally.

Theoretically, BAE stability depends upon the competition between the fast-ion drive and the background damping. Ion Landau damping is one possible damping term. It depends upon the ratio of ion thermal speed-to-wave phase velocity. The ion thermal speed scales as $m_i^{-1/2}$ but so does the expected mode frequency (equation (1)), so ion Landau damping is expected to be insensitive to the species mix. Meanwhile, the fast-ion drive depends upon the slope of the distribution function at the wave-particle resonance. Previous work [7] showed that the deuterium beam ions drive BAEs when recently deposited beam ions satisfy the wave particle resonance condition, $\omega = n\omega_\phi - (m-1)\omega_\theta$ where ω is the BAE frequency in the plasma frame, n and m are the BAE toroidal and poloidal mode numbers, and ω_ϕ and ω_θ are the toroidal and poloidal repetition frequencies of the fast-ion orbits. Figure 7(*a*) shows that this condition is also satisfied during deuterium injection into the mixed-species plasma of figure 6. Interestingly, recently deposited hydrogen ions also satisfy this resonance condition (figure 7(*b*)) but, nevertheless, the hydrogen beams do not drive BAEs unstable. Factors that may contribute to greater hydrogen beam stability include the following. (i) Although the hydrogen and deuterium beam powers

Table 2. Comparison of calculated linear growth rates γ with the pure deuterium baseline case. 'Similar' means changes of $\lesssim 10\%$. The right column summarizes the experimental trends.

Mode	Change	GTC	FAR3d	Experiment
BAE	Thermal H	More unstable	Similar	More unstable
BAE	H NBI	Similar	Similar	More stable
LFM	Thermal H	More unstable	Similar	More unstable

were well matched (lower panel of figure 6), only a single near-tangential source was used during deuterium injection, while two sources (one near-tangential and one near-perpendicular) were employed during hydrogen injection. As a result, the phase-space density of deposited ions in the vicinity of the resonance is lower for the hydrogen injection case. (ii) Another factor is the slowing-down time. For fast ions that slow down on electrons, the slowing-down time is proportional to mass; however, when T_e is large, fast ions slow down primarily on thermal ions, and thermal-ion drag is insensitive to species mix. For the conditions of figure 6, the hydrogen slowing-down time is 82% of the deuterium slowing-down time, so the overall number of hydrogen fast ions is lower. (iii) A final factor is the orbit size, which is $\sim 51\%$ larger for deuterium NBI. The effect of this on the fast-ion drive depends in a rather complicated manner on the mode structure and orbit size [14]. For the passing 80 keV deuterium ions that drive the modes, the gyrodiameter is ~ 5 cm at the BAE mode, the drift-orbit shift is ~ 9 cm, and the radial full-width half-maximum of the mode is ~ 13 cm. In summary, one expects that deuterium beams with a single injection angle should more readily destabilize BAEs than hydrogen beams with multiple injection angles, as experimentally observed. Meanwhile, the main effect of the thermal species is to shift the mode frequency, which can shift the location of resonances in phase space.

Turning to simulation, both the gyrokinetic code GTC [9] and the gyrofluid code FAR3d [11] previously analyzed discharge #178631 (the reference case of the dedicated deuterium experiment) using an isotropic Maxwellian deuterium distribution function to model the fast ions. Here, linear simulations are repeated with a single change in input parameters: the thermal ion mass. Figure 8 summarizes the GTC results. For the $n = 3$ BAE (figure 8(a)), both the growth rate and the frequency decrease with increasing ion mass, with an approximate $1/\sqrt{m_i}$ scaling. For the $n = 3$ LFM (figure 8(b)), the mode frequency hardly changes with increasing mass but the growth rate drops appreciably. The growth rate also drops rapidly with increasing mass for the $n = 6$ LFM but, in this case, the frequency increases $\sim 30\%$ between hydrogen and tritium (figure 8(c)). In FAR3d simulations, replacing the thermal deuterium with thermal hydrogen makes only modest changes in growth rate for modes in both the LFM and BAE bands.

In a second set of simulations, the mass of the fast ions is switched from deuterium to hydrogen with all other parameters left unchanged. In this case, in contradiction to experiment, GTC predicts a slightly higher BAE growth rate with hydrogen injection than with deuterium injection; FAR3d finds a comparable growth rate. The likely explanation for this discrepancy is the use of an isotropic Maxwellian distribution function to model the fast ions. With this model for the fast ions, GTC also fails to reproduce the strong q_{min} dependence of BAE stability in pure deuterium discharges [9], a discrepancy that is also attributed to the difference between an isotropic distribution and the highly anisotropic beam distribution of the experiment.

A qualitative comparison of these linear growth rate calculations with the experimental trends appears in table 2.

4. Summary

In summary, the main findings of the previously published work are the following.

(a) BAE are driven unstable through resonances with high-energy (~ 80 keV) deuterium beam ions.
(b) BAEs are more unstable near rational values of q_{min}.
(c) BAE mode properties are adequately described by established theory.
(d) The modes previously called BAAEs were misidentified—we now call them LFMs.
(e) LFMs are not driven by high-energy fast ions.
(f) LFMs occur near rational values of q_{min} in plasmas with high electron temperature but low beta.
(g) LFMs are probably a low frequency reactive instability of predominately Alfvénic polarization.

The new findings on the isotope dependence are the following.

(a) LFMs are more unstable in mixed-species plasmas than in deuterium plasmas, as predicted by both analytical theory and gyrokinetic simulations.
(b) During deuterium NBI, experimentally, BAEs appear more unstable in mixed-species plasmas, consistent with the modest increase in linear growth rate predicted by GTC.
(c) Experimentally, hydrogen beams did not drive BAE instability, in contradiction to simulations with an isotropic Maxwellian fast-ion distribution.

Acknowledgments

Assistance by the DIII-D team and valuable discussions with Liu Chen are gratefully acknowledged. This material is based upon work supported by the U.S. Department of Energy, Office of Science, Office of Fusion Energy Sciences, using the DIII-D National Fusion Facility, a DOE Office of Science user facility, under Awards DE-FC02-04ER54698, DE-SC0020337, and DE-SC0019352.

ORCID iDs

W.W. Heidbrink https://orcid.org/0000-0002-6942-8043
G.J. Choi https://orcid.org/0000-0003-0044-1650
M.A. Van Zeeland https://orcid.org/0000-0002-7911-2739
G.H. Degrandchamp https://orcid.org/0000-0002-1363-9570
D.A. Spong https://orcid.org/0000-0003-2370-1873
A. Bierwage https://orcid.org/0000-0003-1243-0502
N.A. Crocker https://orcid.org/0000-0003-2379-5814
X.D. Du https://orcid.org/0000-0001-6127-2825
G.R. McKee https://orcid.org/0000-0002-2754-9816

References

[1] Heidbrink W.W., Strait E.J., Chu M.S. and Turnbull A.D. 1993 *Phys. Rev. Lett.* **71** 855
[2] Gorelenkov N.N., Berk H.L., Fredrickson E. and Sharapov S. E. ((JET EFDA Contributors) 2007 *Phys. Lett.* **370** 70
[3] Cheng C.Z., Chen L. and Chance M.S. 1985 *Ann. Phys., NY* **161** 21
[4] Sharapov S.E., Testa D., Alper B., Borba D.N., Fasoli A., Hawkes N.C., Heeter R.F., Mantsinen M. and Von Hellermann M.G. 2001 *Phys. Lett.* **289** 127
[5] Duong H.H., Heidbrink W.W., Strait E.J., Petrie T.W., Lee R., Moyer R.A. and Watkins J.G. 1993 *Nucl. Fusion* **33** 749
[6] Gorelenkov N.N. *et al* 2009 *Phys. Plasmas* **16** 056107
[7] Heidbrink W.W., Van Zeeland M.A., Austin M.E., Crocker N.A., Du X.D., McKee G.R. and Spong D.A. 2021 *Nucl. Fusion* **61** 066031
[8] Heidbrink W.W. *et al* 2021 *Nucl. Fusion* **61** 016029
[9] Choi G.J., Liu P., Wei X.S., Nicolau J.H., Dong G., Zhang W.L., Lin Z., Heidbrink W.W. and Hahm T.S. 2021 *Nucl. Fusion* **61** 066007
[10] Van Zeeland M.A. *et al* 2016 *Nucl. Fusion* **56** 112007
[11] Varela J. *et al* 2018 *Nucl. Fusion* **58** 076017
[12] Lauber P., Günter S., Könies A. and Pinches S.D. 2007 *J. Comput. Phys.* **226** 447
[13] Heidbrink W.W., Miah M., Darrow D., LeBlanc B., Medley S.S., Roquemore A.L. and Cecil F.E. 2003 *Nucl. Fusion* **43** 883
[14] Fülöp T., Lisak M., Kolesnichenko Y.I. and Anderson D. 1996 *Plasma Phys. Control. Fusion* **38** 811